

# Anomalous diffusion in a microtron and critical structure at the chaos boundary

B. V. Chirikov

G. I. Budker Institute of Nuclear Physics, 630090 Novosibirsk, Russia

(Submitted 19 April 1996)

Zh. Éksp. Teor. Fiz. 110, 1174–1185 (October 1996)

This paper describes the results of an investigation of anomalous diffusion in critical structures at order–chaos and chaos–chaos boundaries, involving both numerical experiments and theoretical analysis. In the first case the critical exponent  $c_D$ , which determines the rate of anomalous diffusion through the expression  $D \propto t^{c_D}$ , is measured yielding the result  $c_D \approx 1/3$ . A value of the correlation exponent  $c_A \approx 1/2$  is also found which is in complete agreement with the predictions of the resonance theory of critical phenomena in dynamical systems. The most important result of the paper is a confirmation of the central assumption of this theory, namely that there exists a supercritical local order parameter in the vicinity of the boundary on the side where the motion has a chaotic component. © 1996 American Institute of Physics. [S1063-7761(96)00310-1]

## 1. INTRODUCTION

The microtron was the first cyclic accelerator of relativistic particles invented by Veksler.<sup>1</sup> The dynamical behavior of the microtron energy is approximately given by the simple mapping  $x, p \rightarrow \bar{x}, \bar{p}$  over one period of rotation of an electron in the magnetic field:

$$\bar{p} = p + K \sin x, \quad \bar{x} = x + \bar{p}. \quad (1)$$

Here  $x$  is the phase of the accelerating voltage with amplitude  $V_0$  and frequency  $\Omega$ ; the canonically conjugate action  $p$  and the single parameter  $K$  of the model are related to the energy of an electron  $E$  and  $\omega_B$ , the maximum Larmor frequency, by the following expressions (in a system of units where  $e = m = c = 1$ ):

$$|p| = \frac{2\pi E \Omega}{\omega_B}, \quad K = \frac{2\pi V_0 \Omega}{\omega_B}. \quad (2)$$

The dynamics of the microtron model (1) was studied in Refs. 1 and 2 and by many other authors (see, e.g., Ref. 3). In all these papers, the main focus of attention was on regular acceleration (for which  $|p| \propto t$  holds, where  $t$  is the number of iterations of the mapping (1)), which corresponds to (neutral) stability of the dynamics of the phase  $x$  (i.e., nondecaying oscillations). This microtron acceleration regime is possible only for special values of the parameter  $K = K_n \approx 2\pi n$ , where  $n \neq 0$  is any whole number. The region of stability in  $xp$  phase space is very small, and decreases rapidly with  $n$ —even for the fundamental microtron regime  $|n|=1$  this region occupies less than 1% of the phase space. What happens for the other initial conditions?

Strange as it may seem, many years passed before this question was answered, and only after the simplicity of the Veksler model (1) made it one of the basic models for addressing general questions about nonlinear dynamics and chaos (see, e.g., Refs. 4 and 5). This model is also called the standard mapping, since many other physical problems reduce approximately to it.

It turns out that for  $K > 1$  the dynamics is that of unbounded diffusion ( $|p| \propto \sqrt{t}$ ) over a considerable portion of

the phase space; as  $K$  increases, the region of unbounded diffusion extends over practically the entire plane. In this limit, the microtron is converted to a “stochastron,” a term introduced by Burshtein *et al.*<sup>6</sup> They proposed to create diffusive acceleration by feeding a noise voltage to the system. This goal can also be accomplished by simply changing the initial conditions (slightly) and/or the parameter  $K$  (over wide limits).<sup>7</sup> To this author’s knowledge, neither of these assertions has been proven or even demonstrated experimentally, although in one mode of operation (without microtron regimes), the stellarator<sup>8</sup> uses dynamic chaos to preheat plasmas.

The dynamics of the “simple” model (1), which turns out to be very rich, has been (and continues to be) studied intensively, both theoretically and by numerical experiments. These studies have revealed that the statistical properties of the motion, especially diffusion, can be very unusual, or “anomalous” (see, e.g., Ref. 9). It turns out that this behavior is associated with the phase-space boundary with chaos, in the neighborhood of which the motion develops a very complex hierarchical structure. Although this structure itself has been studied in great detail,<sup>9,10</sup> its influence on the statistical properties of the motion still remains unclear for the most part.<sup>9,11</sup> It is this problem that is the subject of the present paper.

## 2. ISLANDS OF STABILITY

The main regions (“islands”) of the phase plane where the acceleration predicted by model (1) is regular form around the fixed points (periodic solutions)  $p = 0 \pmod{2\pi}$ ,  $x = \pm x_0$ , where

$$K \sin x_0 = 2\pi n, \quad K^2 = s^2 + (2\pi n)^2, \quad s = K \cos x_0, \\ -4 < s < 0. \quad (3)$$

The inequalities determine the region of stability of the fixed points. In what follows we set  $s = -2$  (the center of stability). For each value of  $|n|$  there are two islands per  $2\pi \times 2\pi$  phase space cell. All the islands are similar in the dimensionless variables

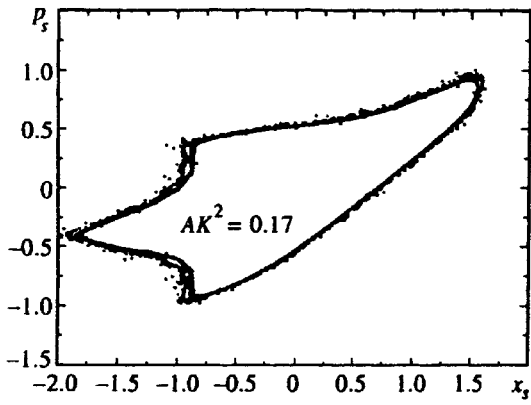


FIG. 1. Universal boundary of the microtron regions in dimensionless variables (4):  $n=2-20000$ ; the duration of the motion for each  $n$  equals 3000 iterations of the mapping (1). The region inside the boundary corresponds to regular motion, while outside it the motion is chaotic. Near the fixed point  $x_s=p_s=0$  the frequency of small oscillations  $\omega_0=\pi/2$ , while at the boundary  $\omega_b=2\pi r_b$  (6).

$$x_s = \frac{x-x_0}{x_b}, \quad Kx_b \approx 0.99, \quad p_s = \frac{p}{p_b}, \quad Kp_b \approx 2.49. \quad (4)$$

Figure 1 shows the boundaries of five islands for  $n=2, 20, 200, 2000, 20000$ . The region of regular motion lies within a boundary of this kind, and the relative area of an island  $A$  is given by the expression

$$AK^2 \approx 0.17. \quad (5)$$

It is noteworthy that the maximum area  $AK^2 \approx 0.19$  is achieved for a stability parameter  $s \approx -1.92$ . All the similarity relations (3)–(5) are obtained from theory,<sup>4,9,11</sup> but their numerical coefficients are empirical. The boundary of an island of stability defines a transition from chaos to order. This boundary is robust, i.e., it is not destroyed by small changes in the single model parameter  $K$ , which is also the order parameter. This follows, in particular, from Eq. (3).

A peculiarity of this model is that although the dimensions of the chaos boundary and the region of regular motion are extremely small, they nevertheless can significantly alter the statistical properties of the chaotic component of the mo-

tion. The explanation for this is that the chaotic trajectories “get stuck” in the complicated critical structure along the chaos boundary.<sup>9,11</sup> This structure is entirely determined by the number of the rotation at the boundary

$$r = r_b = 0.23889\dots = [4, 5, 2, 1, 1, 1, 2, \dots], \quad (6)$$

which is also independent of  $n$ . The last expression (6) gives a representation of  $r$  in the form of a continued fraction (the consecutive elements of the fraction are given in the brackets). Since the rotation number  $r = \omega/2\pi$  is the ratio of the frequency of oscillation to the perturbation frequency ( $2\pi$ ), this representation reveals the basic nonlinear resonances near the boundary, which also determine the critical structure, in a most natural way. These resonances correspond to the convergent sequence of rationals  $r_m = p_m/q_m \rightarrow r$  as  $m \rightarrow \infty$ . Each of the denominators  $q_m$  equals the period of motion of a particular resonance.

A clear picture of the critical structure, which also describes its renormalization group, can be obtained from the spectrum of motion at the boundary, an example of which is shown in Fig. 2a. The spectrum  $S(\nu)$  is obtained from the radial oscillations  $\rho(t)$  (where  $\rho^2 = x_s^2 + p_s^2$ ) perpendicular to the chaos boundary. A characteristic feature of the spectrum is the irregularity of the fundamental peaks, which are labeled by integers  $m$ . The periods of the corresponding resonances are  $q_m = 4, 17, 21, 38, 59, 97, 350, 447, \dots$ , for  $m = 1, 2, 3, 4, 5, 6, 7, 8, \dots$ . This picture, which is typical of a critical structure, is described by the chaotic renormalization group.<sup>9,11</sup> It implies that the change in the structure of the motion in going from one scale to the next is irregular in character, and must itself be described statistically (the dotted line in Fig. 2a). The odd resonances ( $m = 1, 3, 5, 7, \dots$ ) lie within the stable region (inside the chaos boundary), whereas the even resonances envelope the boundary, i.e., they are in the chaotic component of the motion.

For comparison, Fig. 2b shows the special case of exact similarity<sup>10</sup> (the fixed point of the renormalization group), where the transition from scale to scale is regular. It is curious that exact similarity includes both regular and chaotic components of the motion (paths). The motion in both cases is almost periodic (with a discrete spectrum); the finite width

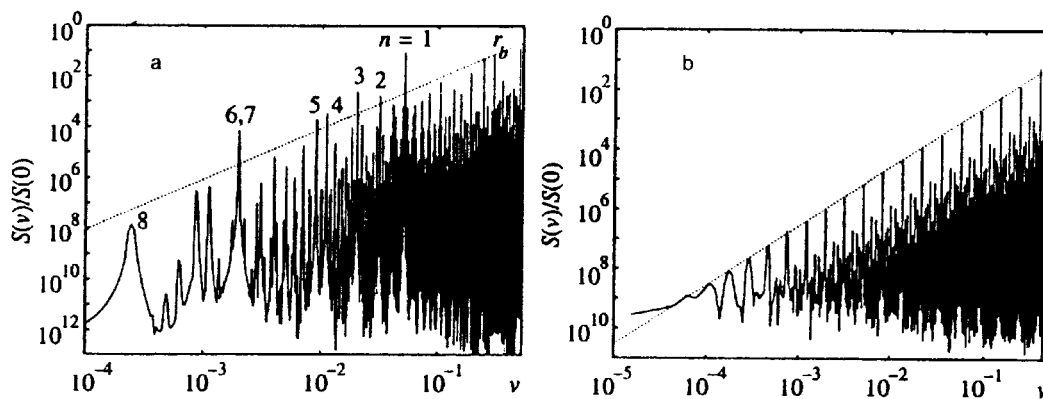


FIG. 2. Example of the spectrum of motion at the chaos boundary: the frequency is  $\nu \pmod{1}$ ,  $S(\nu)/S(0)$  is the relative magnitude of the Fourier amplitude; the total duration of the motions  $T=65536$  iterations. a) Statistical similarity (chaotic renormalization group) at the robust order-chaos boundary:  $n=1$ ;  $r_b=0.23713$  (the peak labelled  $r_b$ ), which differs somewhat from the asymptotic value (6). The numbers on the curve are the labels  $m$  of the fundamental resonances, while the dotted line is the theory (8). b) Exact similarity (fixed point of the renormalization group) at the nonrobust chaos-chaos boundary for the special point  $r_b=(3-\sqrt{5})/2=[2, 1, 1, 1, \dots]$  and  $K=0.9716$ .

of the peaks  $\Delta\nu \sim 1/T$  is determined by the total duration of the motion  $T$ .

### 3. CRITICAL STRUCTURE AND ANOMALOUS DIFFUSION

The main level of the critical structure is determined by a sequence of fundamental nonlinear resonances, each of which consists of a comb of  $q_m$  stable regions around the trajectory of period  $q_m$ , surrounded by a rather thick chaotic layer (for a detailed discussion, see, e.g., Refs. 9–11). The comb runs along the chaos boundary; its transverse size  $\rho_m$  and area  $A_m$  are given by the estimate

$$A_m \sim \frac{A(K)}{q_m^2} \propto \rho_m \propto S_m, \quad (7)$$

where  $A(K)$  is the total area of the island (5) and  $S_m = S(\nu_m)$  is the amplitude of transverse oscillations (wiggling) of the chaos boundary at a frequency  $\nu_m = q_m |r_b - r_m| \sim 1/q_m$ . This implies the following global shape of the spectrum, shown in Fig. 2 by a dotted line:

$$S_m \sim \nu_m^2. \quad (8)$$

Of course, for the case of renormalized chaos (Fig. 2a) this simple dependence expresses only the average behavior of the structure, on which are imposed the strong fluctuations that are general characteristics of critical phenomena.

The rate of diffusion is determined by the statistics of the “sticking” time  $t_m$  at the corresponding scale  $m$ . After averaging over time or over initial conditions (ergodicity), and under the assumption of statistical independence of the various sticking events, we have

$$\langle (\Delta p)^2 \rangle \approx \sum_m (\Delta p)_m^2 \approx K^2 \sum_m t_m^2 N_m + \frac{K^2}{2} C_0(K)t. \quad (9)$$

Here  $N_m(t)$  is the number of times the trajectory arrives at scale  $m$  within the full duration of the motion  $t$ ; the last term describes ordinary diffusion (with an additional coefficient  $C_0(K) \sim 1$  due to close correlations), which occupies the overwhelming portion of the time due to the smallness of the regular region in the problem under discussion. In turn, the number of arrivals is given by

$$N_m = t P_m, \quad P_m \sim A/t_m^{c_P}, \quad (10)$$

where  $P_m = P(t_m)$  is the distribution of Poincaré returns, i.e., the distribution over time of delays during reflection (scattering) from the chaos boundary. This statistic is characterized by a critical exponent  $c_P$ . From the ergodicity of the motion it follows that

$$\frac{t_m N_m}{t} = t_m P_m = A_m \sim \frac{A}{q_m^2} \sim \frac{A}{t_m^{c_A}}. \quad (11)$$

The function  $A_m = A(t_m)$  plays the role of the correlation of sticking events; from the last estimate above (similarity) we have  $c_P = c_A + 1$ . This implies an asymptotic average rate of diffusion

$$D(t) \equiv \frac{\langle (\Delta p)^2 \rangle}{t} \rightarrow K^2 \sum_m t_m A_m \sim AK^2 t_{\max}^{1-c_A} \sim AK^2 (At)^{c_D}, \quad (12)$$

where the critical exponent of the diffusion equals

$$c_D = \frac{1 - c_A}{1 + c_A}, \quad (13)$$

and the maximum sticking time  $t_{\max}$  is determined from the condition

$$N_m(t_{\max}) \sim \frac{At}{t_{\max}^{c_P}} \sim 1, \quad \left( \frac{t_{\max}}{t} \right)^{c_P} \sim \frac{A}{t^{c_A}} \ll 1. \quad (14)$$

The sum in (12) reduces approximately to the largest term  $t_m = t_{\max}$ , because all the quantities that describe of the critical structure depend exponentially on the scale label  $m$  (a geometric progression). Of course, this is true only for  $c_A < 1$ . In the opposite case the rate of diffusion does not depend on time, i.e., it is normal.

The theory of critical exponents at the chaos boundary turns out to be far from trivial. In order to calculate these exponents, it is necessary to estimate the quantity  $t_m(q_m)$ . At first glance, it is natural to assume  $t_m \sim q_m$ , i.e., that the (un)sticking time is the same order as the characteristic time for this scale.<sup>12</sup> However, it is immediately clear from (7) and (14) that this would imply  $c_A = 2$ , together with  $c_P = 3$ , which is completely inconsistent with the reliably measured value of the exponent  $c_P \approx 1.5$ .<sup>9,11,13,14</sup> In addition to this quantitative discrepancy, this assumption would imply a qualitatively different kind of diffusion,<sup>11</sup> i.e., one that is normal in spite of the sticking of trajectories.

This qualitative effect is particularly important for evaluating the elaborations of the work of Ref. 12 presented in Ref. 15. In this approach, attention is focused primarily on the interior of the chaos boundary, which also has a hierarchical structure (“resonances around resonances;” see also Refs. 16 and 17). A value of the critical exponent  $c_P$  can be successfully obtained using this method that is very close to the empirical value  $c_P \approx 2$ ;<sup>15</sup> this value still excludes anomalous diffusion. Meanwhile, it was shown in Ref. 9 that for  $c_P < 2$  the contribution of the interior of the chaos boundary generally has no effect on the critical exponents.

Nevertheless, it should be noted that the scale  $t_m \sim q_m$  has a definite physical meaning, not only dynamically (the period of the fundamental resonance) but also statistically, in that it determines the rate of local diffusion  $D_l \sim q_m^{-4}/q_m = q_m^{-5}$  perpendicular to the chaos boundary.<sup>18</sup> This type of diffusion has actually been observed recently;<sup>16</sup> however, it is bounded and leads only to establishment of local statistical equilibrium without any movement to neighboring scales.

In order to resolve this contradiction, the authors of Ref. 11 advanced the hypothesis that at the critical point we have  $t_m = \infty$ , i.e., all scales of the critical structure are dynamically isolated and separated by their chaotic boundaries, which are invariant curves. In view of the hierarchical nature of the critical structure, the latter form an everywhere-dense set. According to this hypothesis, finite values of  $t_m$  are explained by the departure of the local order parameter near the

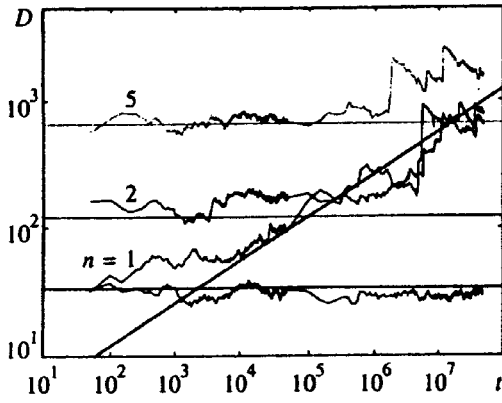


FIG. 3. Anomalous diffusion for model (1) in the microtron regime (3): the broken curves are numerical data for  $n=1, 2, 5$  and a control count with  $K=2\pi$  (see text); the horizontal lines show (constant) rates of normal diffusion. The oblique line is the function (19) with the theoretical value  $c_D=1/3$  and empirical value  $b=11$  (for  $n=1, M=40$ ).

chaos boundary from its critical value at the boundary itself. In this case, from one side of the boundary the structure becomes subcritical, which ensures regular motion for the majority of initial conditions, whereas from the opposite side supercritical structure arises with a finite sticking time. Under the assumption that the local order parameter depends linearly on the distance to the chaos boundary, we obtain the estimate

$$t_m \sim q_m^{c_i}, \quad c_A = 2/c_i. \quad (15)$$

Depending on the details of the critical structure,  $c_i=7$  (Ref. 11) or  $c_i=4$  (Ref. 9), and accordingly  $c_A=2/7$  or  $c_A=1/2$ . The latter value is considered to be more precise (see the discussion in Ref. 9).

In both cases we have  $c_A < 1$ , which leads to anomalous (accelerated) diffusion ( $c_D > 0$ ). In point of fact, the first numerical experiments<sup>11</sup> have already confirmed the existence of anomalous diffusion at the chaos boundary, and consequently disprove both the initial assertion  $c_i=1$  of Ref. 12 and its further elaboration in Ref. 15. This type of diffusion has been investigated in many subsequent papers (see, e.g., Refs. 17, 19, and 20).

Note that while there are many general studies of anomalous diffusion, both accelerated ( $c_D > 0$ ) and retarded ( $c_D < 0$ ), that predate the present paper (see, e.g., Ref. 21), the topic of interest here is diffusion connected with the specific critical structure at the chaos boundary.

#### 4. NUMERICAL EXPERIMENTS

A fundamental problem with the empirical study of anomalous diffusion in this model arises from large fluctuations. The latter are, in turn, explained by the fact that the main contribution to the diffusion (for a given segment of time) comes from the single sticking event with  $t_m = t_{\max}$ . For this reason, fluctuations grow with time (Fig. 3). In order to suppress them a doubled average is used: first average  $D(t)$  over  $M=40$  independent trajectories, and then average the critical exponent  $c_D(t)$  over four groups of trajectories, also independent.

The basic results of the numerical experiments are shown in Fig. 3 for  $n=1, K_1=6.5938\cdots, D_0=C_0K^2/2 \approx 39$ ;

$n=2, K_2=12.72\cdots, D_0 \approx 121$ ; and  $n=5, K_5=31.47\cdots, D_0 \approx 644$ . For comparison the case of normal diffusion with  $K_0=2\pi$  is also shown. In this case the stable region is completely disrupted (see (3)), and despite the insignificant change in  $K$  ( $K_1/K_0-1 \approx 0.05$ ), the diffusion remains normal for all choices  $t \leq 5 \cdot 10^7$  of the number of iterations of the mapping (1).

The existence of anomalous diffusion is not in doubt. With regard to measurement of the critical exponent  $c_D$ , matters are more complicated due to the strong fluctuations mentioned above. Figure 3 clearly shows the "Levy jumps"<sup>21</sup> associated with sticking of the trajectories at the chaos boundary. It is interesting that the steepness of these jumps is distinctly asymmetric—a peculiarity whose mechanism is not fully clear. The asymptotic regime of anomalous diffusion is reached after a certain time that increases with the size of the islands. Plots of the asymptotic function  $D(t)$  ( $t > t_a$ ) on a log-log scale can be fitted by the linear expression (see (12)):

$$\ln D(t) = c_D \ln t + \ln B. \quad (16)$$

As a result, the following values are obtained:

$$n=1, \quad c_D=0.29-0.37, \quad B=4.4-1.3,$$

$$t_a=5 \cdot 10^3-10^5, \quad n=2, \quad c_D=0.34-0.39,$$

$$B=2.2-0.9, \quad t_a=5 \cdot 10^4-5 \cdot 10^5. \quad (17)$$

The minimum value  $t_a$  used in the fit is determined by passing to the asymptotic regime, while the maximum is bounded by the large jumps in  $D(t)$  (see Fig. 3). Although anomalous diffusion is clearly evident even for  $n=5$ , practical counting times turn out to be insufficient to reach the asymptotic regime, at least for an accurate measurement of  $c_D$ . The values of  $c_D$  obtained for  $n=1,2$  in (17) are in good agreement with each other and with the theoretical value  $c_D=1/3$ , which is used to plot the straight line shown in Fig. 3. According to (12), the second fitting parameter  $B$  can be represented in the form

$$B_n = b A_n K_n^2 (A_n M)^{c_D} \approx \frac{0.07 b M^{1/3}}{n^{2/3}}, \quad t^{c_A} \geq f M A_n, \quad (18)$$

where  $A_n$  now denotes the total area of the two islands of stability for a given  $n$ , and  $b, f$  are certain constants. The dependence on the number of trajectories  $M$  arises from the fact that for anomalous diffusion it is sufficient that any one of the trajectories stick, provided that the last inequality (18) holds. In the opposite case, we have  $t_m \sim t$  and  $c_D \approx c_A \approx 1/2$ . In this case, it is  $t$  that enters into the inequality and not  $Mt$ , since the trajectories are independent. The last expression for  $B_n$  in (18) was obtained by taking (5) into account and using the value  $c_D=1/3$ . For  $M=40$  the values (17) imply  $b \approx 11$  ( $n=1, B \approx 2.8$ ) and  $b \approx 10$  ( $n=2, B \approx 1.5$ ). The final expression for the coefficient of anomalous diffusion is the following:

$$D_a(t) \approx 0.76 (Mt/n^2)^{1/3}, \quad (19)$$

which is plotted in Fig. 3 (the oblique straight line) for  $n=1$ .

Let us now compare these results with known data. First of all, the rather large theoretical value  $c_D=1/2$  given in Ref. 22 is explained by the simplifying assumption  $t_{\max} \sim t$  (compare (14)) adopted in Ref. 22 and taken from Refs. 9 and 11. This assumption is valid only when inequality (18) is violated, in particular, for very large  $M$  and small  $t$  (see below).

Anomalous diffusion at a chaos boundary was probably first observed in the numerical experiments of Ref. 23 for exactly this model with  $n=1$ . However, the rate of diffusion was given only for the maximum counting time  $t=10^8$ . For some reason, the authors of Ref. 23 were unable to observe anomalous diffusion for  $n=2$ , although for  $t=10^8$  its rate is the same as for  $n=1$ , which is still much larger than the normal rate:  $D/D_0 \approx 7.3$  (see (19) for  $M=64$  and Fig. 3). For  $n=1$ , the ratio  $D/D_0 \approx 27$  found in Ref. 23 is in satisfactory agreement with the average  $D/D_0 \approx 36$  of (19), taking into account the large fluctuations also noted in Ref. 23.

In Ref. 20 data were presented on anomalous diffusion for the same model, but over a very short time interval  $t \leq 2000$  and for a somewhat different value of  $K=6.9115$ , for which the area of the stable region is decreased by a factor of 5. The critical exponent was taken to equal  $c_D=1/3$ ; however, the accuracy of this value is unknown, primarily due to the smallness of  $t$ . For the maximum counting time we have  $D \approx 160$ , whereas the theoretical value (19), taking into account the small area of the islands (see (18)) is  $D \approx 60$ . The difference is probably related not so much to fluctuations as to the change in the shape of the islands of stability, and accordingly the rotation number at the boundary with chaos. It is interesting to note that an enormous number of trajectories  $M=10^5$  was used in this paper to calculate the distribution function for anomalous diffusion (see also Ref. 17). Therefore, these results also provide indirect confirmation of the dependence of the average rate of diffusion on  $M$  (19), which at first glance is strange. Without this factor, the rate would fall by almost a factor of 50! More detailed analysis of the data of Ref. 20, which was verified by additional numerical experiments, shows that for  $t \sim 100$  a transition occurs from  $c_D \approx 0.5$  to  $c_D \approx 0.3$ , most likely related to violation of the inequality (18). From this follows the estimate  $f \sim 0.05$ .

Similar results are also obtained from the different (continuous-time) model of Ref. 17, with  $M=3600$  and a maximum  $t \sim 10^5$  (in comparable units). In particular, the critical exponent  $c_D \approx 0.38 \approx 1/3$  remains roughly the same despite the completely different global structure of the motion. This provides additional confirmation of the universality of the critical structure at the chaos boundary. Note that in this model the decrease of  $c_D$  at counting times around  $t \sim 10^4$  is even more obvious (see Fig. 7 in Ref. 20) and corresponds to roughly the same value of  $f$  for  $A \sim 1$ .

Thus, the existence of anomalous diffusion due to the critical structure at the chaos boundary can be regarded as firmly established. However, at this time both the demonstration of existence of anomalous diffusion itself (i.e.,  $c_D > 0$ ) and the approximate computation of the critical exponents are possible only within the resonance theory of critical structure of chaos, with the additional hypothesis of the dynamic separation of scales.<sup>9,11</sup> This important hypothesis can

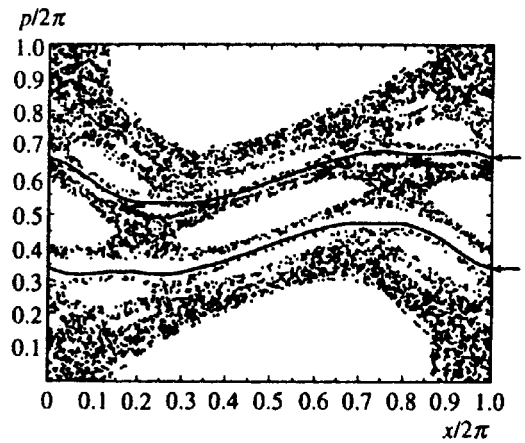


FIG. 4. Phase portrait of model (1) for the critical value  $K=0.9716\dots$ . The arrows show the two chaos-chaos boundaries that separate the chaotic components. Motion in each of these regions is represented by a single trajectory using  $t=10^7$  iterations with step size  $\Delta t=2000$  and  $5000$ .

be verified further, at least qualitatively, by using a different model with a chaos-chaos boundary.

## 5. STATISTICAL PROPERTIES OF MOTION AT A CHAOS-CHAOS BOUNDARY

In contrast to the better-known and more robust order-chaos boundary, which is preserved over a relatively wide range of variation of the order parameter ( $K$  in our model), the chaos-chaos boundary is not robust, i.e., it is destroyed by any deviation from the critical value  $K=0.9716\dots$ .<sup>10</sup> Figure 4 shows a phase portrait of the model (1) for this case. The critical invariant curves shown by arrows are absolute barriers to the motion; however, chaotic trajectories can approach arbitrarily closely to them from both sides. Because the local order parameter is now supercritical on both sides of the boundary, its decrease as the boundary is approached becomes at least quadratic; of course, the supercriticality rapidly decreases while the sticking time grows rapidly. This in turn leads to a decrease in the critical correlation exponent  $c_A \rightarrow 0$ , and causes the exponent for anomalous diffusion to increase to its limiting value:  $c_D \rightarrow 1$ . The first confirmation of this structure at the chaos-chaos boundary was obtained in Ref. 11 by measuring the statistics of Poincaré returns (10): The critical exponent  $c_p = 1 + c_A \approx 0.975 \pm 0.013$  actually turns out to be very close to its limiting value.

Figure 5 shows the results of measurements of anomalous diffusion in this case. The average rate of diffusion along  $x$  is defined as

$$D_x(t) = \frac{\langle (\Delta x)^2 \rangle}{t} \approx B t^{c_D}, \quad \Delta x = \sum_i [p(t) - p_r]. \quad (20)$$

Here the resonance value of the momentum  $p_r = p_1 = 0$  during diffusion for an integer resonance (below the lower boundary in Fig. 4) and  $p_r = p_2 = \pi$  for diffusion at a half-integer resonance (between the two boundaries).

In this case the mapping (1) corresponds to a different physical model—the motion of particles in a multiwave field. The variables  $x, p$  are now Cartesian, with unbounded variation of the coordinate  $x$ . This is the type of model investi-

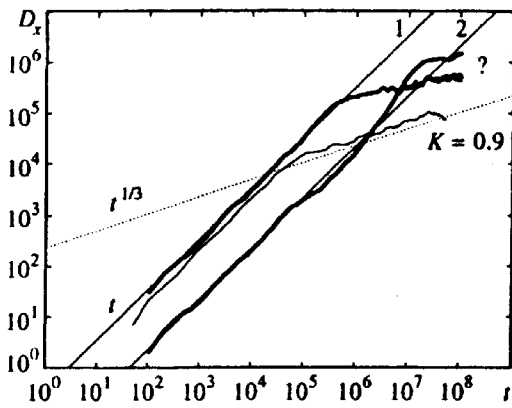


FIG. 5. Anomalous diffusion at a chaos-chaos boundary: model (1) with critical value  $K=0.9716\dots$ , averaging over  $M=100$  independent trajectories. The heavy curves correspond to diffusion with the limiting rate  $D(t) \propto t$  (steep lines) for integer ( $t$ ) and half-integer resonance (2). For comparison, diffusion for the subcritical value  $K=0.9$  is also shown (light curve); the dotted line corresponds to  $c_D=1/3$  for diffusion at the chaos-order boundary.

gated in Ref. 17 for the two-wave case. Although this case is the simplest from a physical point of view, it turns out to be considerably more complicated from the standpoint of numerical experiments and theoretical analysis.

It is clear from Fig. 5 that the diffusion exponent  $c_D \approx 1$  actually increases rapidly and is close to its limiting value. If the trajectories were to get stuck near the chaos boundary for the entire duration of the motion  $t$ , then the coefficient in (20) would be  $B_i \approx (2\pi r_i)^2$ , where  $r_1 = (3 - \sqrt{5})/2 \approx 0.382$  is the number of rotations at the lower chaos boundary, while  $r_2 = 0.5 - r_1$ . From this we have  $B_1 \approx 5.8$  and  $B_2 \approx 0.55$ . In fact, from the data shown in Fig. 5 it follows that  $B_1 \approx 0.35$ ,  $B_2 \approx 0.023$ , i.e., it is approximately 20 times smaller. This is most likely connected with the relatively small size of the intrinsically critical structure ( $A \sim 0.1$ ; compare the parameter  $f$  of the same order in inequality (18)). On the other hand, this area is still considerably larger than in the microtron model, which is probably the main reason for the considerable decrease in fluctuations (compare Figs. 3 and 5). In any case, the small value of the coefficient  $B$  shows that it is diffusion that occurs, and not regular motion along  $x$ , although both mechanisms give  $x \propto t$ . This is also confirmed directly by observation outside the trajectories. In particular, this quasiregular motion along  $x$  takes place on both sides! For  $c_P \approx 1$  and  $c_A \approx 0$ , inequality (18) is already violated for  $M \gtrsim 1/f \sim 10$ , and the rate of diffusion does not depend on  $M$ . In both cases  $c_D \approx (1 - c_A)/(1 + c_A) \approx 1 - c_A \approx 1$ .

Thus, the diffusion limit at a chaos-chaos boundary actually confirms the hypothesis of supercriticality, which is very important for further development of the theory of critical phenomena in dynamic systems. However, the nature of the stable (i.e., independent of initial conditions for the trajectories) anomaly for large  $t \gtrsim 10^6$ , demonstrated by curve 1 in Fig. 5 with particular force, remains completely unclear. Traces of this anomaly were already noted in Ref. 11, based on the more rapid decay of the distribution function of Poincaré returns  $P(t)$  when  $t \gtrsim 10^5$ . This anomaly also turns out

to be stable and is not connected with small statistics, as proposed in Ref. 11.

Outwardly, the anomaly in Fig. 5 appears to indicate that the value of the parameter  $K=0.9716$  is still subcritical (compare the case  $K=0.9$ ), or that for some reason the sticking takes place away from the fundamental chaos-chaos boundary at one of the interior chaos-order boundaries. On the other hand, no anomalies are seen in the spectrum of motion at the chaos-chaos boundary (Fig. 2). On the whole, this question requires a separate investigation of its own.

## 6. CONCLUSION

An extensive series of numerical experiments has been conducted in order to study critical structures at a chaos-order boundary (Fig. 1) for the simple dynamic system (1). The study is based on observing the very distinctive anomalous diffusion (Fig. 3) caused by this structure. In particular, accurate measurements have been made of the value of the critical exponent  $c_D \approx 1/3$  appearing in the expression (12) for anomalous diffusion that is predicted by the resonance theory of critical phenomena.<sup>9,11</sup> The investigations were made in the special (microtron) regime (3) of model (1), at which the chaos boundary has a very small size (Fig. 1). Despite this, the statistical properties of all the chaotic components of the motion were fully determined by using a sufficiently large time interval. This work emphasizes the importance of critical phenomena in dynamics, especially with regard to the robustness (structural stability) of the chaos-order boundary.

One of the main goals of this study was to confirm the underlying hypothesis of the theory regarding the supercritical nature of the local order parameter with respect to the chaotic component in the vicinity of the boundary. The empirical value of  $c_D$  and the value of the critical correlation exponent at the chaos boundary  $c_A \approx 1/2$  (see (13)) obtained from it completely confirm this hypothesis. In view of its importance for the theory as a whole, an additional verification was undertaken using a different (critical) value of the order parameter  $K=0.9716\dots$ , at which a (nonrobust) chaos-chaos boundary appears in the system with a qualitatively different structure (Figs. 1, 2, and 4). The rapid increase in  $c_D \rightarrow 1$  and decrease in  $c_A \rightarrow 0$  predicted by the theory are actually confirmed (Fig. 5). Nevertheless, a stable anomaly was observed (also noted in Ref. 11) which is under study at this time. It is interesting to note that in this case the rate of (homogeneous) diffusion reaches its limiting value  $|\Delta x| \propto t$ , i.e., the motion is similar to that of a free particle, but that it takes place at a lower rate, and from both sides of the boundary!

This work was carried out by the Russian Fund for Fundamental Research (Grant 95-01-010047).

<sup>1</sup>V. I. Veksler, Dok. Akad. Nauk SSSR 43, 346 (1944).

<sup>2</sup>A. A. Kolomenskiĭ, Zh. Tekh. Fiz. 30, 1347 (1960) [Sov. Phys. Tech. Phys. 5, 865 (1960)].

<sup>3</sup>S. P. Kapitsa and V. N. Melekhin, *The Microtron*. Nauka, Moscow, 1969 [in Russian].

<sup>4</sup>B. V. Chirikov, Phys. Rep. 52, 263 (1979).

<sup>5</sup>R. Z. Sagdeev, D. A. Usikov, and G. M. Zaslavskiĭ, *Nonlinear Physics: from the Pendulum to Turbulence and Chaos*, Harwood Academic, New

- York (1988); A. Lichtenberg and M. Lieberman, *Regular and Chaotic Dynamics*. Springer, 1992.
- <sup>6</sup>É. L. Burshtein, V. I. Veksler, and A. A. Kolomenskiĭ, in *Some Problems in the Theory of Circular Accelerators*, p. 3. USSR Acad. Sci. Publ., Moscow, 1955 [in Russian].
- <sup>7</sup>G. M. Zaslavskii and B. V. Chirikov, *Usp. Fiz. Nauk* **105**, 3 (1971) [*Sov. Phys. Usp.* **14**, 549 (1971)].
- <sup>8</sup>V. N. Bocharov, V. I. Volosov, A. V. Komin *et al.*, *Zh. Tekh. Fiz.* **40**, 1334 (1970) [*Sov. Phys. Tech. Phys.* **15**, 1033 (1970)].
- <sup>9</sup>B. V. Chirikov, *Chaos, Solitons, and Fractals* **1**, 79 (1991).
- <sup>10</sup>R. MacKay, *Physica D* **7**, 283 (1983).
- <sup>11</sup>B. V. Chirikov and D. L. Shepelyansky, *Physica D* **13**, 395 (1984).
- <sup>12</sup>J. Hanson, J. Carry, and Y. Meiss, *J. Stat. Phys.* **39**, 327 (1985).
- <sup>13</sup>B. V. Chirikov and D. L. Shepelyanskiĭ, *Proc. 9th Intl. Conf. on Nonlinear Oscillations*, Vol. 2, p. 420 (Kiev, 1981). Naukova Dumka, Kiev, 1984 [in Russian].
- <sup>14</sup>C. Karney, *Physica D* **8**, 360 (1983).
- <sup>15</sup>J. Meiss and E. Ott, *Phys. Rev. Lett.* **55**, 2741 (1985); *Physica D* **20**, 387 (1986).
- <sup>16</sup>S. Ruffo and D. L. Shepelyansky, *Phys. Rev. Lett.* **76**, 3300 (1996).
- <sup>17</sup>G. M. Zaslavskii and S. S. Abdullaev, *Phys. Rev. E* **51**, 3901 (1995).
- <sup>18</sup>B. V. Chirikov, *Lect. Notes Phys.* **179**, 29 (1983).
- <sup>19</sup>H. Mori, H. Hata, T. Horita, and T. Kobayashi, *Prog. Theor. Phys. Suppl.* **99**, 1 (1989).
- <sup>20</sup>R. Ishizaki, H. Hata, T. Horita, and H. Mori, *Prog. Theor. Phys.* **84**, 179 (1990); *Prog. Theor. Phys.* **85**, 1013 (1991).
- <sup>21</sup>P. Levy, *Théorie de l'Addition des Variables Eleatoires*. Gauthier-Villiers, Paris, 1937; T. Geisel, J. Nierwetberg, and A. Zacherl, *Phys. Rev. Lett.* **54**, 616 (1985); R. Pasmanter, *Fluid Dynam. Res.* **3**, 320 (1988); G. M. Zaslavskii, M. Yu. Zakharov, A. I. Neishtadt *et al.*, *Zh. Eksp. Teor. Fiz.* **96**, 1563 (1989) [*Sov. Phys. JETP* **69**, 885 (1989)]; R. Voss, *Physica D* **38**, 362 (1989).
- <sup>22</sup>B. V. Chirikov, *Proc. Roy. Soc. Lond. A* **413**, 145 (1987).
- <sup>23</sup>C. Karney A. Rechester, and R. White, *Physica D* **4**, 425 (1982).

Translated by Frank J. Crowne